Electronic Supplementary Material (ESI) for Physical Chemistry Chemical Physics.
This journal is © the Owner Societies 2021

Supporting Information

Probing the shear viscoelasticity of a nanoscale ionic liquid meniscus

Sangmin An[1,2†], Manhee Lee[3†], and Wonho Jhe[1*]

[1]*Department of Physics & Astronomy, Seoul National University, Seoul 08826, Korea*

[2]*Department of Physics, Research Institute of Physics and Chemistry, Jeonbuk National University, Jeonju 54896, Korea.*

[3]*Department of Physics, Chungbuk National University, Cheongju, Chungbuk 28644, Korea*

†S.A. and M.L. contributed equally.
*E-mail: whjhe@snu.ac.kr

Supplementary Note

Negative shear elasticity in the nano-bridges of ionic liquids

In dynamic force microscopy of AFM, the measured interaction force is decomposed into the effective elastic force F_k and damping force F_b. The force components can be further represented by the elastic and damping constants, such as $k_{int} = F_k / A$ and $b_{int}w = F_b / A$, where A is the oscillating amplitude and w (=2πf) is the angular frequency. While it is clear that the positive-valued damping constant b_{int}, as observed in experiment, originates from the friction between the tip surface and the liquid, the negative-valued k_{int} seems to be counter-intuitive at a first glance. The negative-valued elastic constant k_{int} is due to the inertial effect of the fluid [S1]. By solving the Navier-Stokes equation for the confined fluid, here the liquid bridge, one can obtain the total force experienced by the tip [S2], $F_{int} = -(1+i)\cot[((1-i)h/\delta)\kappa x]$, where h is the confining height of fluid, x the oscillating amplitude of the tip, and δ and κ are the characteristic constants of the fluid-oscillator systems (Refs. [S2]). The corresponding force constants, k_{int} and b_{int}, are obtained from the in-phase and the out-of-phase components of the total interaction [S1,S2], where the elasticity k_{int} is shown to exhibit the negative value and decreases down to $-\sigma w^{3/2}\sqrt{\eta\rho/2}$ (σ is the contact area) with increase of the confining height. Using the parameters of our system, tip radius of 100 nm, density (η) of 1.21 g/mL, viscosity (η) of 150 mPa·s, the negative-valued elasticity, $-\sigma w^{3/2}\sqrt{\eta\rho/2}$, gives about -0.0015 N/m, which is comparable to the experimentally observed elasticity, -0.002 N/m.

References

[S1] M. Lee, B. Kim, Q. Kim, J. Hwang, S. An, and W. Jhe. Viscometry of single nanoliter-volume droplets using dynamic force spectroscopy. *Phys. Chem. Chem. Phys.* **18**, 27684 (2016).

[S2] M. Lee, J. Hwang, B. Kim, S. An, and W. Jhe. Fluid-induced resonances in vibrational and Brownian dynamics of a shear oscillator. *Curr. Appl. Phys.* **16**, 1459 (2016).

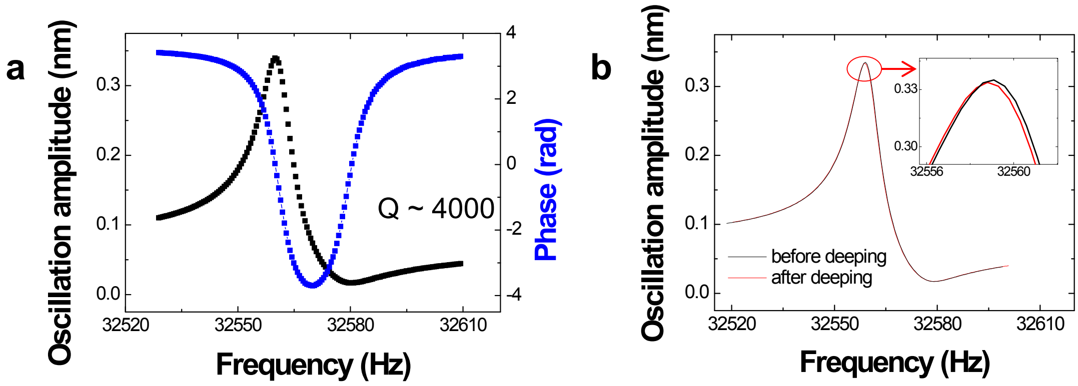

Figure S1 | Quality (*Q*-) factor of the QTF sensor tip. (a) Resonance curve of the tip - The *Q*-factor of the QTF sensor is ~4,000 with amplitude of ~0.33 nm at the resonance frequency of 32,560.6 Hz. The tip experiences the interaction forces by approaching the surface and forms an ionic liquid (IL) bridge between the tip and the substrate. **(b) Resonance frequency shift by adding a small amount of IL to the surface of the tip apex after dipping it in the bulk IL solution** - We measure the resonance curves of the QTF signals before and after dipping. The resonance frequencies shift is about 0.06 Hz, the quality factors are the same (~4,000) before and after dipping, and the associated mass change is estimated to be ~10^{-11} g.

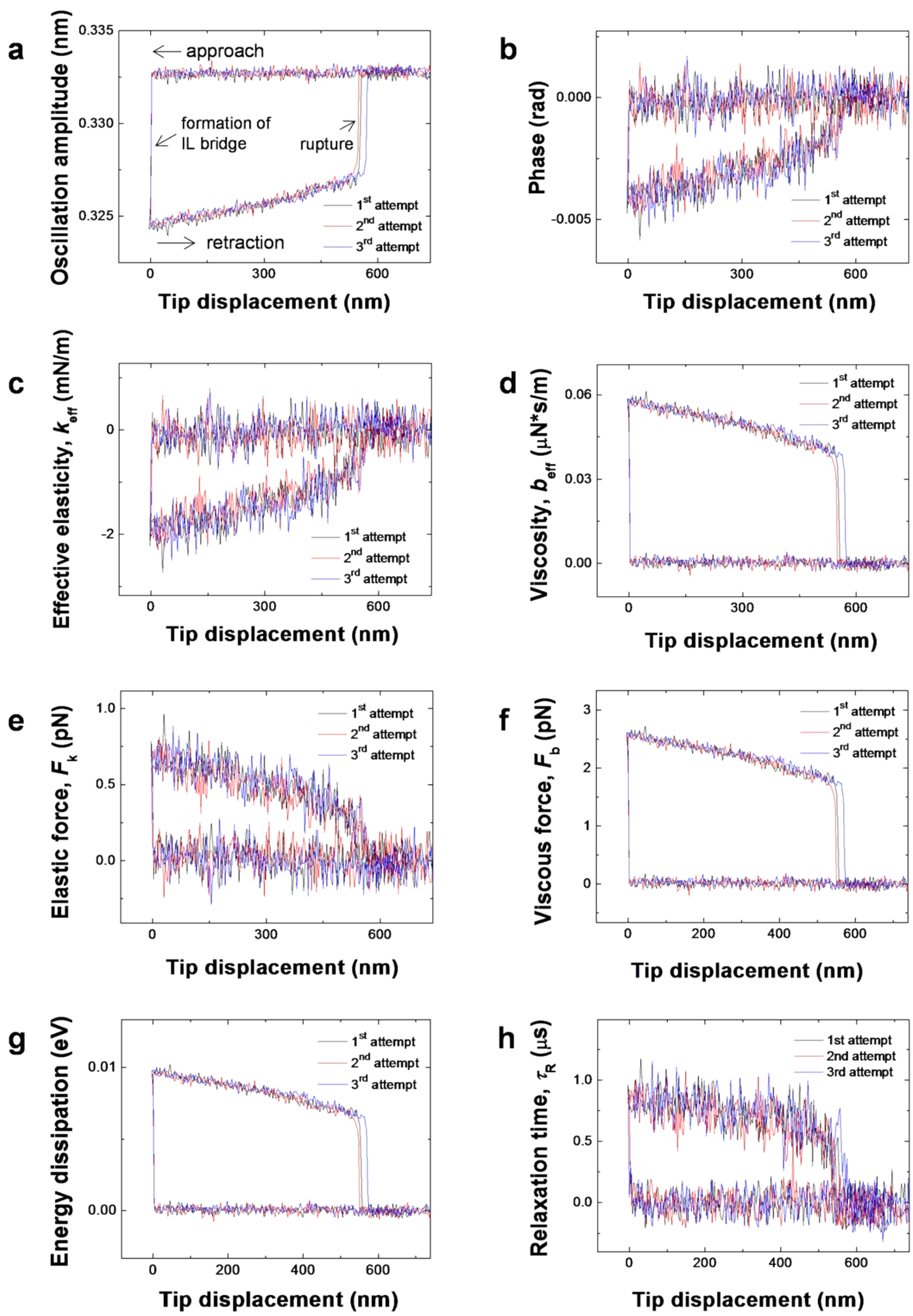

Figure S2 | Bulk IL bridge response from approach/retraction curves for reliable measurement check. The effective elasticity (k_{eff}) **(c)** and viscosity (b_{eff}) **(d)**, the elastic and viscous forces (F_k & F_b) **(e-f),** and the dissipated energy (E_{dis}) **(g)** obtained by the measured values of oscillation amplitude **(a)** and phase **(b)** with respect to the z-axis displacement by using the theory of frequency-modulation (FM) QTF-based AFM [S3, S4]. In addition, the relaxation time (τ_R) **(h)** is calculated from the ratio of elastic and viscous responses by the viscoelastic Maxwell model [S5] as $\tau_R = k_{eff}/(b_{eff}\omega^2)$, where ω is the angular frequency of tip oscillation.

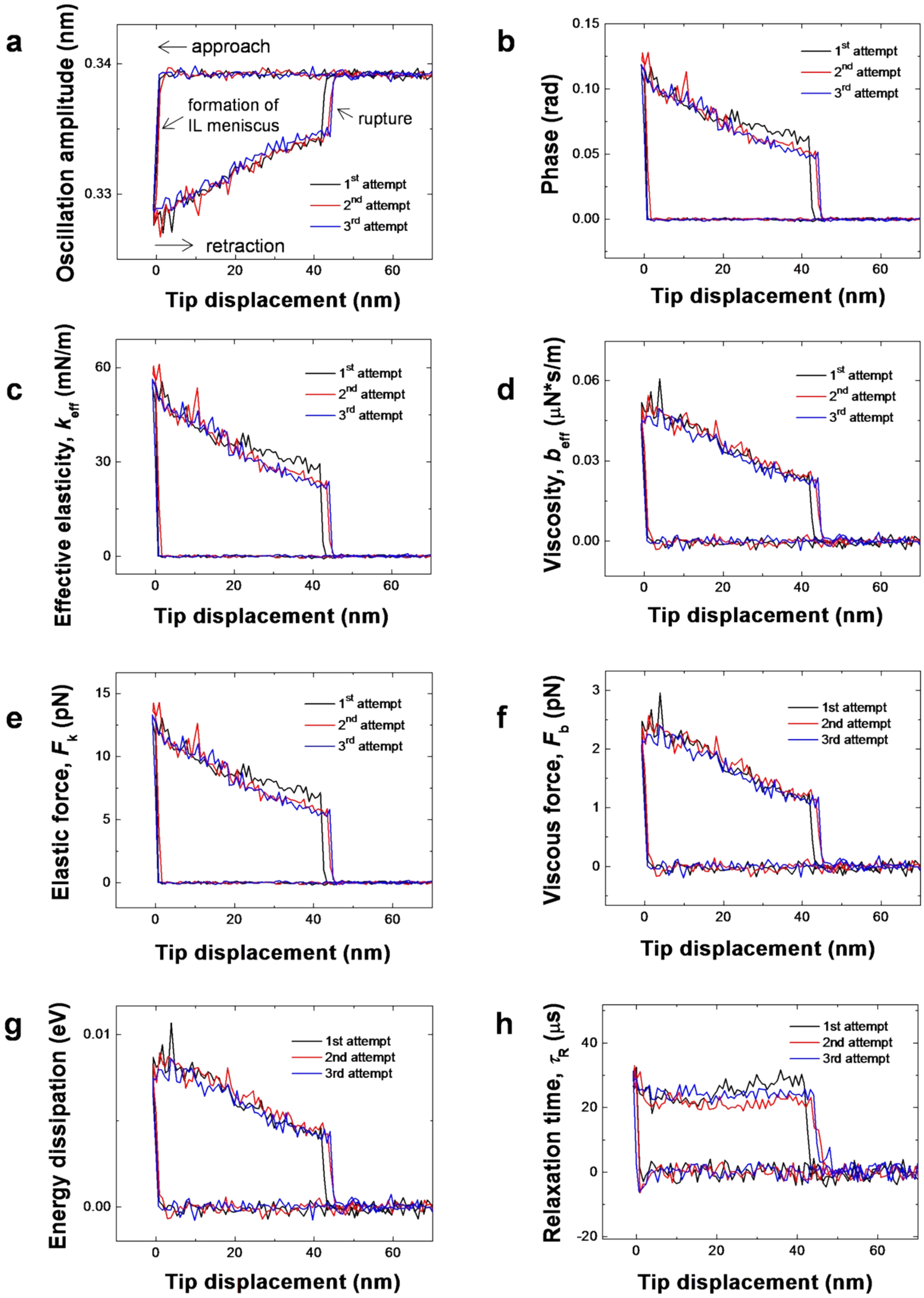

Figure S3 | Nanoscale IL meniscus response from approach/retraction curves. k_{eff} and b_{eff} **(c-d),** F_{k} & F_{b} **(e-f),** and E_{dis} **(g)** obtained by the measured values of amplitude and phase **(a-b)**. τ_R **(h)** is calculated from the ratio of elastic and viscous responses. The value of τ_R is maintained constant until the meniscus ruptured.

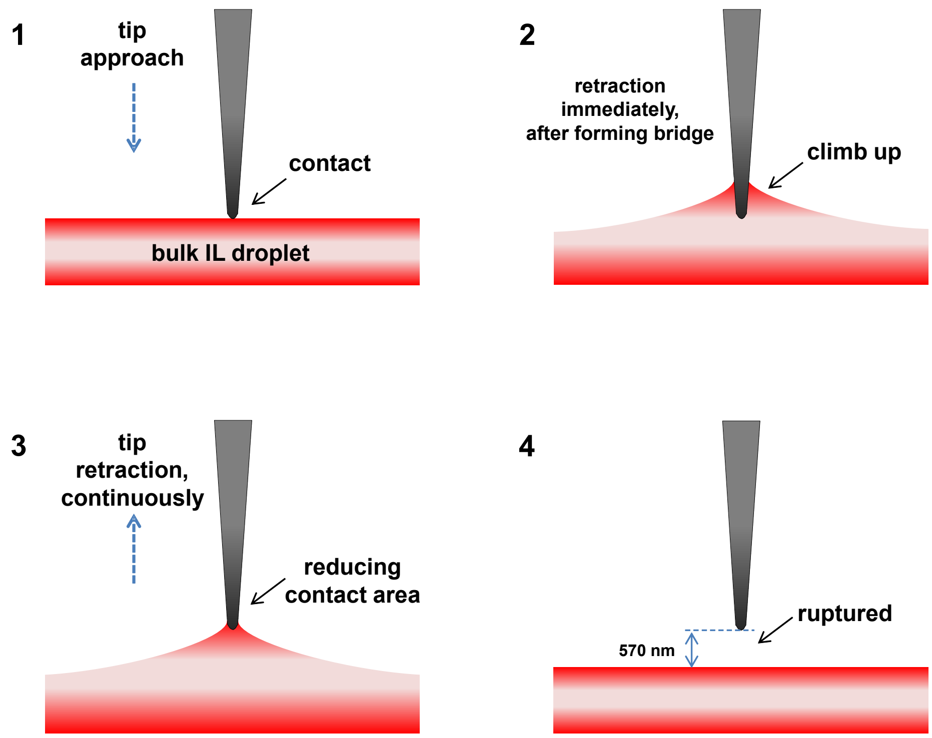

Figure S4 | Long distance rupture of the bulk IL bridge. (1) As the tip approaches and contacts the surface, **(2)** the surface of bulk IL jumps up the apex wall of the sharp tip. The tip immediately retracts and the contact area between the IL and apex wall is gradually reduced by continuous retraction. **(4)** Finally, at approximately 570 nm between the tip and surface, the bridge is ruptured.

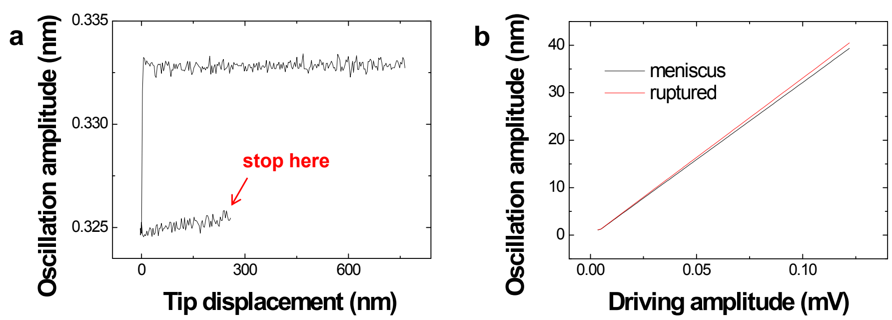

Figure S5 | Shear dynamics of the bulk IL bridge. (a) Shear dynamics of the bulk IL bridge - Shear responses by increment of the oscillation amplitude. After formation of a bulk IL bridge, the tip immediately retracts and stops at 280 nm. Then **(b)** we increase the oscillation amplitude of the tip. The amplitude shows almost linear behaviour even we increase the driving voltage up to 100 times.

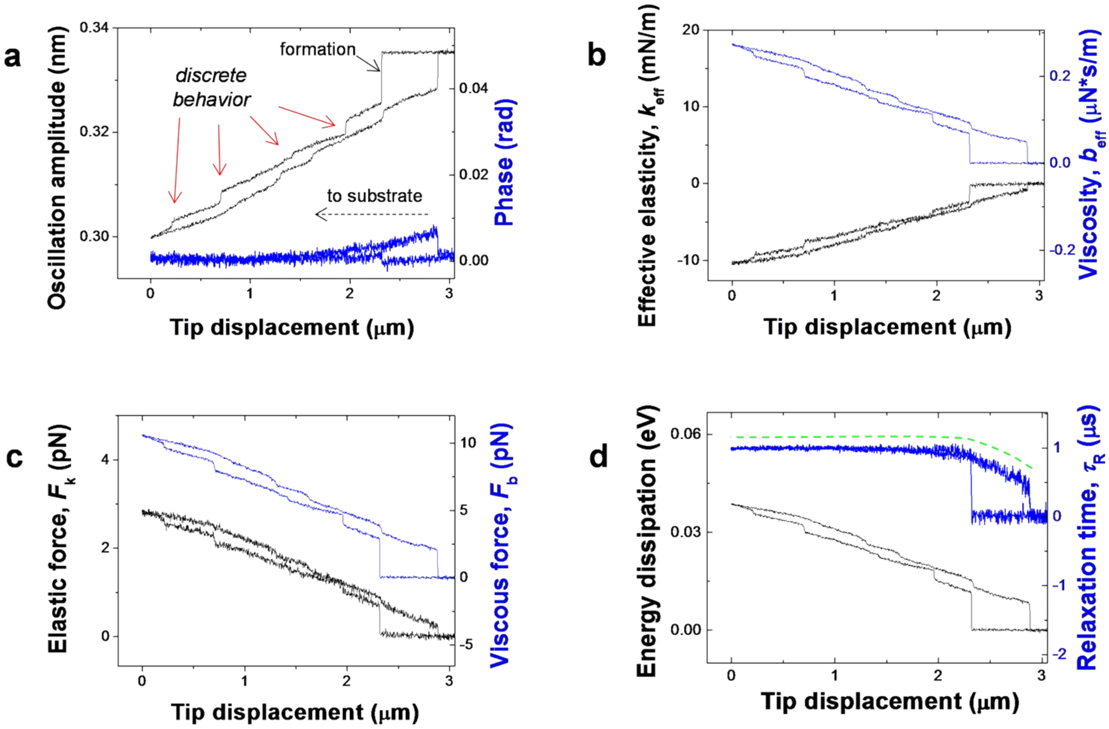

Figure S6 | Excessive dipping-induced shear dynamics of the bulk IL bridge. We further dip the tip into the IL droplet. Interestingly, discrete behaviours show up as the tip enters the bulk IL droplet at a distance of ~400 nm, and we calculate their viscoelastic responses of k_{eff} & b_{eff} **(b),** F_k & F_b, **(c)**, and E_{dis} **(d)** using the amplitude and phase signals **(a)**. Note that k_{eff} in the case of bulk IL shows a negative value during the dipping process, indicating the fluid follows the Maxell liquid model. In addition, we also obtain τ_R **(d)** derived from the viscoelastic responses, which shows a constant value (~1 μs) during continuous dipping and begins to decrease gradually until rupture occurs during tip retraction.

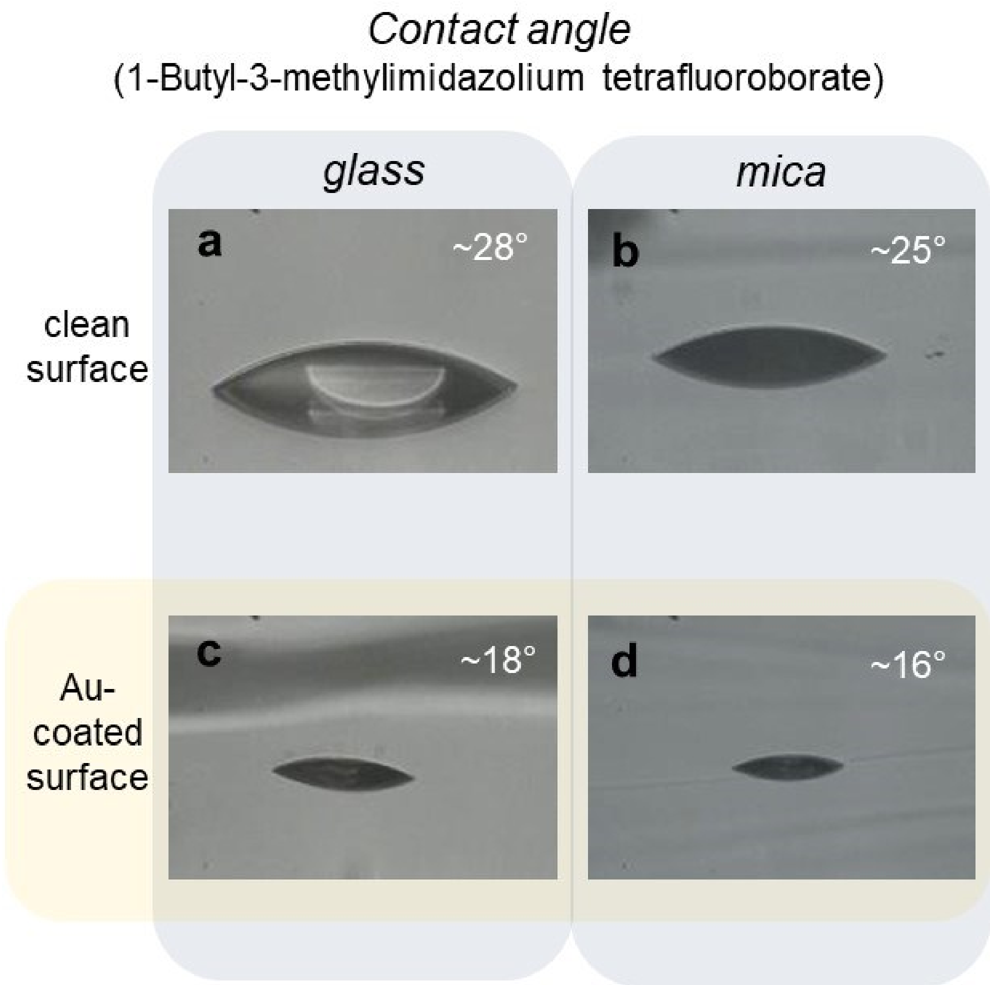

Figure S7 | Contact angle measurement of IL (1-Butyl-3-methylimidazolium tetrafluoroborate). The contact angle was about 28° for droplets of the IL on clean glass (a) and about 25° on mica (b), about 18° on Au-coated glass (c), and about 16° on Au-coated-mica (d).

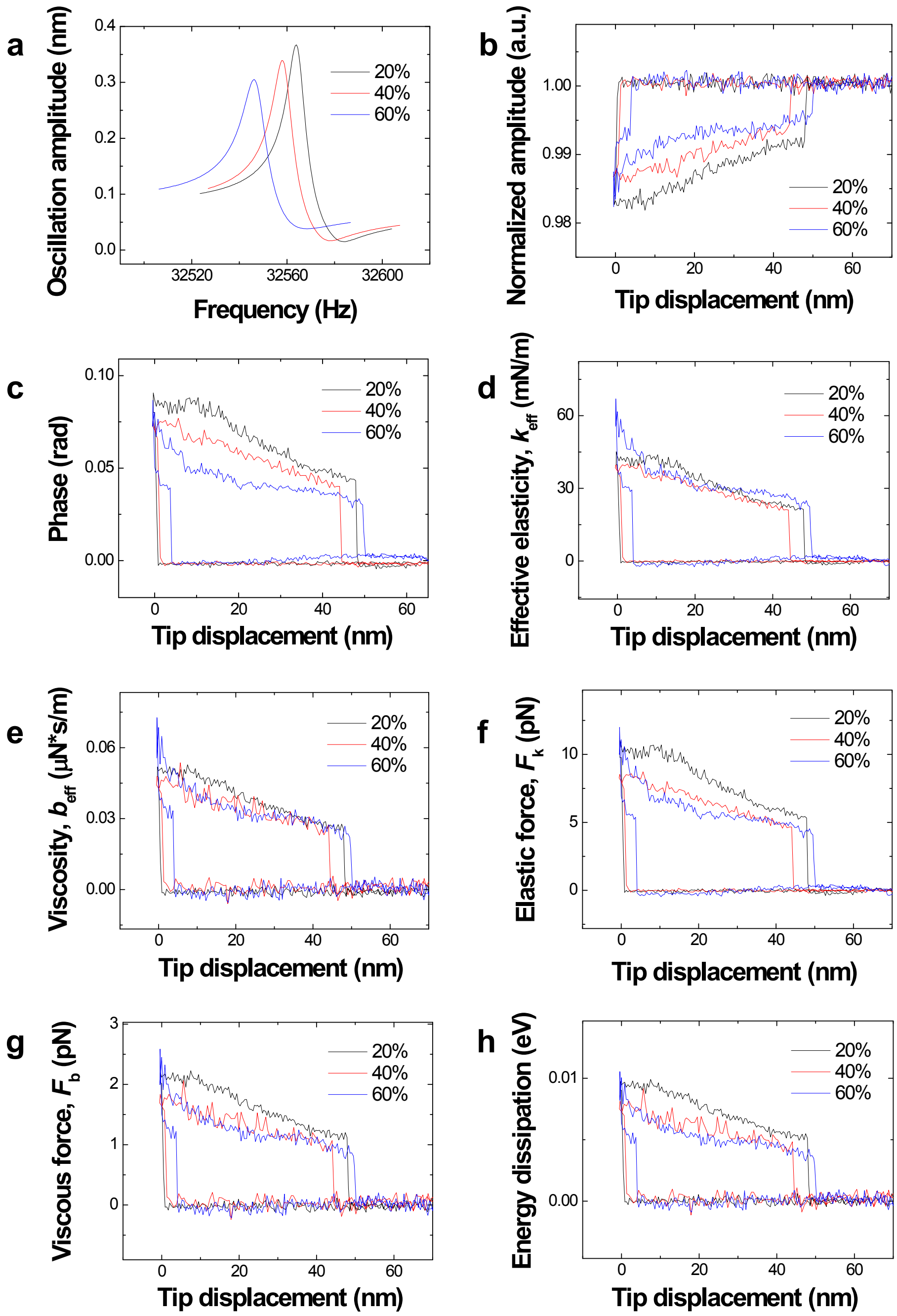

Figure S8 | Humidity dependence of the nanoscale IL meniscus. We check the humidity dependence of the mechanical properties of the nanoscale IL meniscus formed between the tip and the surface for 20%, 40%, and 60% relative humidity. **(a)** Resonance curves of the tip at each relative humidity - Due to mass adhesion of water molecules on two prongs of the QTF, the resonance frequency decreases, and damping exerts on the oscillator as the relative humidity increases. k_{eff} and b_{eff} **(d-e)**, F_k & F_b **(f-g)**, and E_{dis} **(h)** are obtained using the measured values of oscillation amplitude and phase **(b-c)**. No critical variation with respect to humidity is observed.

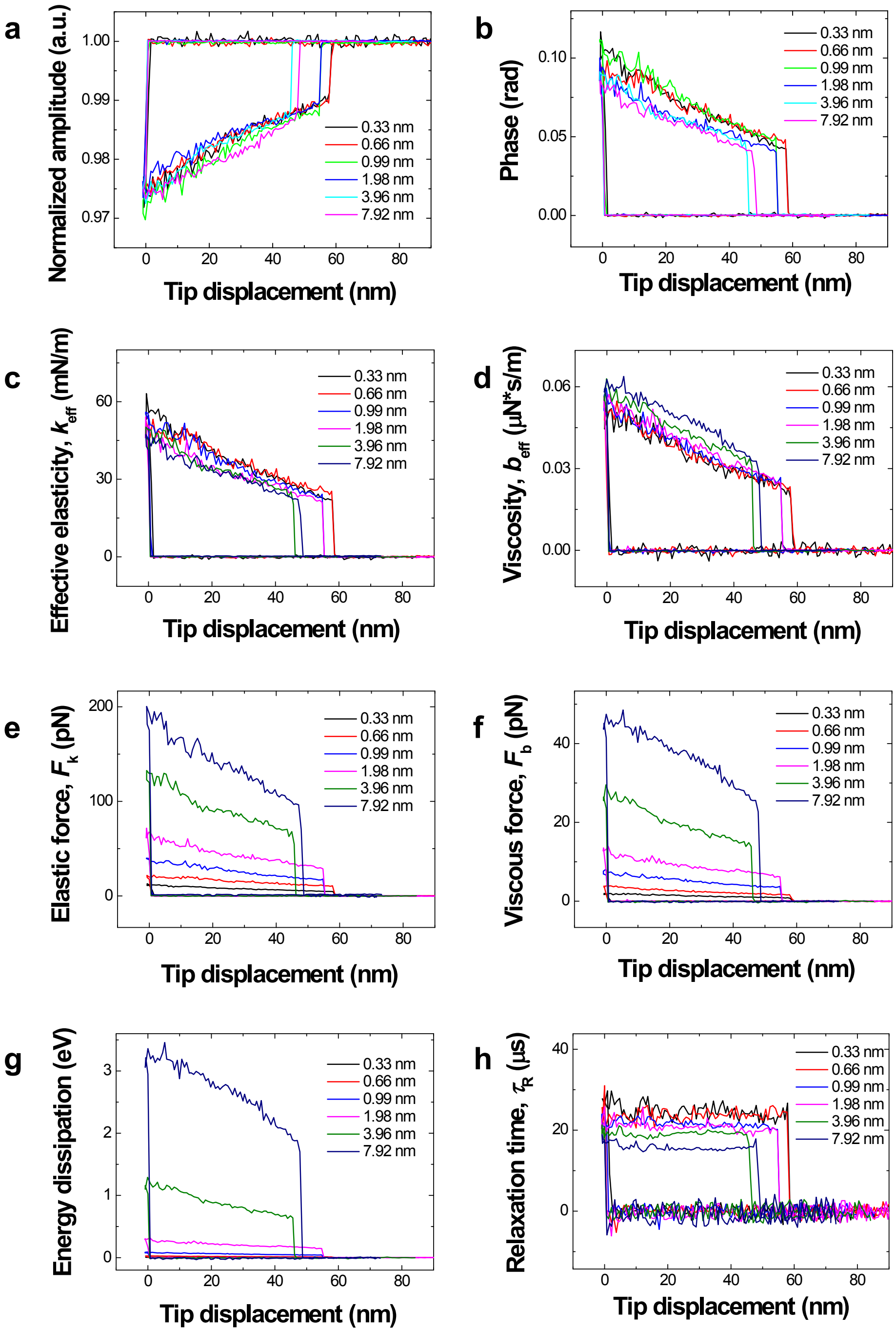

Figure S9 | Shear velocity (v) dependent mechanical response of the nanoscale IL meniscus. Approach/retraction curves of k_{eff} & b_{eff}, **(c-d)**, F_k & F_b **(e-f)** and E_{dis} **(g)** which is calculated using the measured values of the oscillation amplitude and phase **(a-b),** the amplitude from 0.33 nm to 7.92 nm, equivalently corresponding to the velocity v from 0.07 mm/s to 1.62 mm/s. **(h)** The relaxation time does not much change during the retraction of the tip.

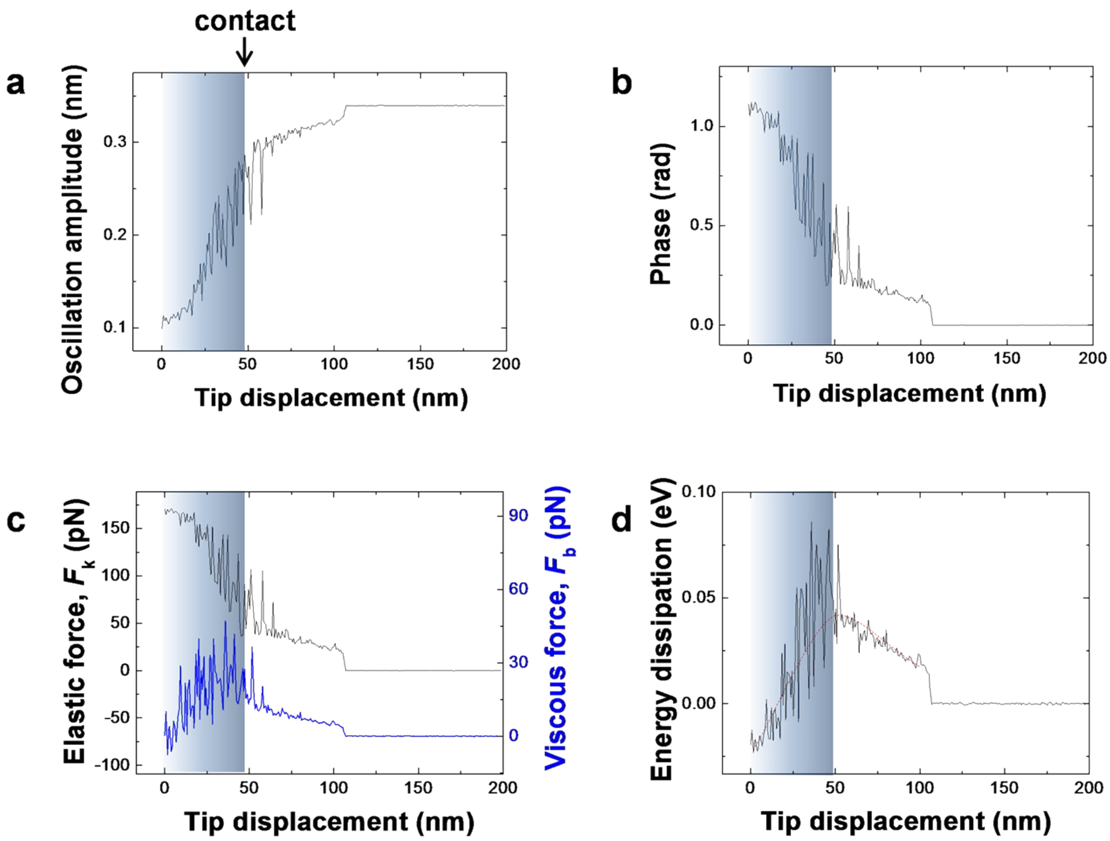

Figure S10 | Determination of the contact point or the surface. After we form a nanoscale IL meniscus, the tip is approached closer to the surface to determine the contact point, at which the slopes of amplitude (a) and phase (b) curves begin to change noticeably, along with the slopes elastic and viscous forces (c) and the energy dissipation (d) at the same time. After we determine the contact point, we perform approach/retraction measurements to investigate the mechanical responses of the nanoscale IL meniscus near the surface by immediately retracting the tip (see the main text accompanying Fig. 4).

References

[S3] M. Lee, J. Jahng, K. Kim and W. Jhe, Quantitative atomic force measurement with a quartz tuning fork, *Appl. Phys. Lett.,* 2007, **91**, 023117.

[S4] M. Lee and W. Jhe, General theory of amplitude-modulation atomic force microscopy, *Phys. Rev. Lett.,* 2006, **97**, 036104.
[S5] R. Lakes, *Viscoelastic Materials*, Cambridge University Press, New York, 2009.